

Spectral shaping with low resolution signals

Hela Jedda, Amine Mezghani and Josef A. Nossek
Institute for Circuit Theory and Signal Processing
Technische Universität München, 80290 Munich, Germany
E-Mail: {hela.jedda, amine.mezghani, josef.a.nossek}@tum.de

Abstract— We aim at investigating the impact of low resolution digital-to-analog converters (DACs) at the transmitter and low resolution analog-to-digital converters (ADCs) at the receiver on the required bandwidth and the required signal-to-noise ratio (SNR). In particular, we consider the extreme case of only 1-bit resolution (with oversampling), where we propose a single carrier system architecture for minimizing the spectral occupation and the required SNR of 1-bit signals. In addition, the receiver is optimized to take into account the effects of quantization at both ends. Through simulations, we show that despite of the coarse quantization, sufficient spectral confinement is still achievable.

I. INTRODUCTION

The ever increasing requirements for higher capacity radio networks makes it important to be able to provide very easily installed, high capacity, low power RF-node solutions. The deployment of a large number of antennas and the access to more bandwidth are considered as key enablers to achieve higher data rates in future wireless networks [1], [2]. To this end, mm-wave communication is a very attractive technology, which provides access to a vast amount of spectrum in the mm-wave band [2], [3], [4]. Due to the smaller wavelength, more antennas can be packed in the same volume as compared to current microwave communication systems, and hence, we come upon arrays with large number of antennas at the base stations, i.e. the so-called massive MIMO [5]. However, there are several issues that need to be addressed for the implementation of massive MIMO in practice. One of the major limiting factors for the implementation of massive MIMO are the complexity issues and the energy consumption due to the large amount of antennas [6]. In particular, high resolution ADCs/DACs with high sampling rate (several Gsps) will require extremely high power consumption and cost, which makes their usage for massive MIMO with individual ADC/DAC for each antenna unbearable. A potential solution to handle this bottleneck is the utilization of low cost and low power RF components [7], such as low resolution, for instance 1-bit, ADCs and DACs together with low complexity modulation (e.g. QPSK). In fact, the analysis of the quantization process has gained a lot of attention in the academic research due to its practical relevance [8], [9], [10], [11], [12], [13], [14]. The front-end structure of transmitters and receivers equipped with a larger number of antennas can be significantly simplified by employing such low resolution devices. In addition, the quantization loss can be compensated partially by increasing the sampling rate. In the case of a 1-bit ADC/DAC, we point out, that there are significant benefits in terms of relaxation for the automatic gain control and requirements on the amplifiers. However, practical concepts of designing low cost and efficient 1-bit transceivers are still an open

research area. While signal processing and communications with 1-bit ADCs have gained recently increased interest by the research community, signal preprocessing for 1-bit DACs is still not well established.

In addition to the spatial processing for beamforming and multi-user processing, appropriate waveform designs are needed to confine and separate the transmitted spectra. Two different approaches, namely multicarrier and single carrier transmission, are commonly studied and considered in the literature in the context of MIMO transmission. On the one hand, multicarrier systems provide a natural solution to the frequency selectivity of propagation channels, which simplifies their equalization. This is very attractive for ultra-wide band channels which are subject to multipath propagation. Filter bank based multicarrier systems (FBMC) offer a number of benefits over conventional orthogonal frequency division multiplexing (OFDM) with cyclic prefix (CP). One benefit is the improved spectral efficiency by not using a redundant CP and by having much better control of out-of-band emission. This is made possible by using optimized prototype filters and more elaborate equalization concepts compared to the single-tap per-subcarrier equalizer (Eq) for OFDM with CP. Another advantage is the large flexibility of choosing the number of sub-carriers without affecting the spectral efficiency, which is a very crucial option to cope with the effects of PAPR, hardware limitations (DAC/ADC, HPA,...) and fast channel variations. For lower frequencies, multicarrier techniques may still be interesting, as long as the number of subcarriers is kept rather low, just to implement channel aware scheduling. Alternatively, single carrier transmission with an appropriate waveform generated by a pulse shaping filter (implemented in the frequency domain or time domain) might be also an attractive solution for higher frequencies due the prominent advantage of lower PAPR compared to multicarrier systems at the cost of additional processing complexity. Nevertheless, both approaches, especially the multicarrier approach are likely to be affected heavily by a low resolution DAC. In fact, under severe quantization, single carrier transmission seems to be more appropriate. Therefore, we aim here at considering the impact of one-bit oversampled DACs on the spectral shape and bandwidth occupation as well as the uncoded bit error ratio (BER) in single carrier. The main idea is to construct and analyze a modulation and waveform design technique having compact spectra and being compatible with low complexity transmitter and receiver implementations (e.g. low resolution ADC/DAC). In addition a receiver design taking into account the effects of quantization will be also presented.

Simulation results show that good performance can be

obtained when optimizing the parameters of the pulse shaper (PS) (like roll-off factor and fractional delay) as well as the receiving filter taking into account the effects of the quantization. In particular, we observed a kind of trade-off between the bandwidth occupation and the required SNR to achieve a certain BER.

Notation: Bold letters indicate vectors and matrices, non-bold letters express scalars. The operators $(\cdot)^*$, $(\cdot)^T$ and $(\cdot)^H$ stand for complex conjugation, the transposition and the Hermitian transposition, respectively. The $n \times n$ identity matrix is denoted by \mathbf{I}_n . \mathbf{C}_{xy} denotes the covariance matrix between the vectors \mathbf{x} and \mathbf{y} . \mathbf{K}_{xy} is defined as the inverse square-root of the diagonal matrix containing only the diagonal elements of the covariance matrix \mathbf{C}_{xy} , i.e. $\mathbf{K}_{xy} = \text{diag}(\mathbf{C}_{xy})^{-1/2}$.

II. SYSTEM MODEL

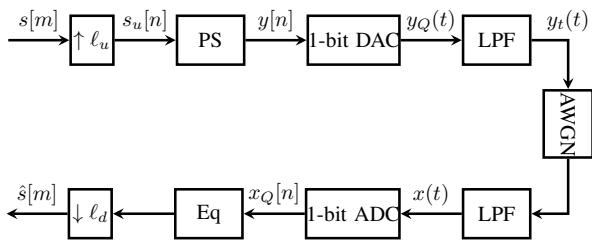


Fig. 1

SINGLE CARRIER COMMUNICATION SYSTEM

Consider the block diagram of a communication system transmitting QPSK symbols generated at a symbol period of T_s depicted in Fig. 1. In the transmitter, the QPSK symbols $s[m]$ from $\mathcal{CN}(0, \sigma_s^2)$ are shaped by a PS in the digital domain at a sample distance of $T = T_s/\ell_u$. The resulting baseband signal is converted to the analog domain, utilizing two 1-bit DACs for the inphase and quadrature components. The inphase and quadrature parts of the input signal $y[n]$ are quantized and mapped to either $+1$ or -1 depending on their signs and then converted to the continuous-time domain by sample and hold method. The low-pass filter (LPF) removes the DACs' alias spectra. The output signal $y_t(t)$ of transmit power P_T propagates through an AWGN channel between the transmitter and receiver and gets disturbed by some Gaussian distributed noise of power spectral density N_0 . The signal-to-noise ratio (SNR) is then defined as $\text{SNR} = \alpha \frac{P_T}{\sigma_n^2}$, where α represents the constant channel power gain and $\sigma_n^2 = N_0/T_s$. The signal captured by the receiver antenna filtered by a LPF to limit the noise bandwidth. The baseband signal is converted into discrete-time domain and then is quantized using two 1-bit ADCs for the inphase and quadrature components. After the ADCs, the Eq filters the received signal to recover the desired signal s . Finally, the signal gets downsampled to obtain the symbols $\hat{s}[m]$ at the symbol rate. In this work, we investigate the design of the PS and the Eq in the time domain when using 1-bit DAC and ADC.

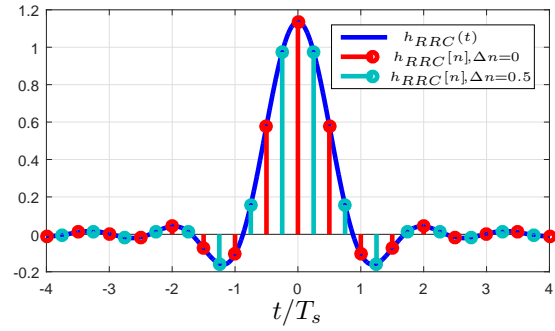


Fig. 2

DIFFERENT DISCRETE-TIME RRC IMPULSE RESPONSES FOR DIFFERENT FRACTIONAL DELAY VALUES Δn : $\rho = 0.5$.

III. DESIGN IN THE TIME DOMAIN

A. Pulse shaper design

The commonly used PS is the root-raised cosine (RRC). The continuous-time RRC impulse response is given by

$$h_{RRC}(t) = \frac{4\rho \cos(\pi \frac{t}{T_s}(1 + \rho)) + \sin(\pi \frac{t}{T_s}(1 - \rho))}{\pi \frac{t}{T_s}(1 - (4\rho \frac{t}{T_s})^2)},$$

where ρ denotes the roll-off factor. Since the PS is processed in digital domain we need an expression for the RRC in discrete-time domain. We get it by sampling the continuous impulse response as follows

$$h_{RRC}[n] = \sum_{n=-\infty}^{+\infty} h_{RRC}(t) \delta(t - (n + \Delta n)T), n = 0, \dots, L_{ps},$$

where $\delta(t)$ is the unit impulse function and $0 \leq \Delta n < 1$. By varying the fractional delay Δn we employ the sampling operation at different time instances so that we get a different discrete-time RRC impulse response for each Δn as depicted in Fig. 2. In addition, the 1-bit DAC is a non-linear function, since its output is simply the sign of the input. And here the question arises: which discrete-time RRC impulse response, i.e. which fractional delay Δn , does lead to the best performance of the non-linear communication system in terms of the spectrum confinement at the transmitter output and the required SNR at the uncoded BER of 10^{-3} ?

B. Equalizer design

The time-domain Eq is denoted by $\mathbf{w} = [w[0], \dots, w[L_{eq} - 1]]$. For simplicity we choose the MMSE Eq that is expressed as

$$\mathbf{w} = \mathbf{e}_\nu^T \mathbf{C}_{x_{qs}}^H \mathbf{C}_{x_q}^{-1},$$

where ν is the delay introduced by the Eq. Since 1-bit quantization is employed in our system model, we have to consider the resulting distortions in the Eq design. To this end, we introduce the following equations that summarize the distortions of the 1-bit quantization introduced to a Gaussian distributed complex-valued signal. Let us assume that \mathbf{r} is the input of the 1-bit quantizer and \mathbf{r}_Q is the output.

We get

$$\begin{aligned} \mathbf{C}_{\mathbf{r}_Q} &= \frac{4}{\pi} (\arcsin(\mathbf{K}_r \Re\{\mathbf{C}_r\} \mathbf{K}_r) + j \arcsin(\mathbf{K}_r \Im\{\mathbf{C}_r\} \mathbf{K}_r)) \\ &\simeq \frac{4}{\pi} \left(\mathbf{K}_r \mathbf{C}_r \mathbf{K}_r + \underbrace{\left(\frac{\pi}{2} - 1\right) \mathbf{I}}_{=c} \right) \end{aligned} \quad (1)$$

$$\mathbf{C}_{\mathbf{r}_Q \mathbf{r}} = \sqrt{\frac{4}{\pi}} \mathbf{K}_r \mathbf{C}_r. \quad (2)$$

The approximation (1) holds true for the assumption $\arcsin(x) \simeq x$.

After using (1) and (2) in the Eq calculations, we end up with the following MMSE Eq expression

$$\begin{aligned} \mathbf{w} &= \mathbf{e}_v^T \mathbf{C}_{\mathbf{x}_Q \mathbf{s}}^H \mathbf{C}_{\mathbf{x}_Q}^{-1}, \\ \mathbf{C}_{\mathbf{x}_Q} &= \frac{4}{\pi} (\mathbf{K}_x \mathbf{C}_x \mathbf{K}_x + c \mathbf{I}), \\ \mathbf{C}_x &= \frac{4}{\pi} (\mathbf{H}_a \mathbf{K}_y \mathbf{C}_y \mathbf{K}_y \mathbf{H}_a^H + c \mathbf{H}_a \mathbf{H}_a^H) + \ell_d \sigma_n^2 \mathbf{\Gamma} \mathbf{\Gamma}^H, \\ \mathbf{C}_y &= \mathbf{H}_{ps} \mathbf{C}_{s_u} \mathbf{H}_{ps}^H, \\ [\mathbf{C}_{s_u}]_{ij} &= \begin{cases} \sigma_s^2 & \text{if } i = j = k \ell_u, k \in \mathcal{N} \\ 0 & \text{else,} \end{cases} \\ \mathbf{C}_{\mathbf{x}_Q \mathbf{s}} &= \frac{4}{\pi} \mathbf{K}_x \mathbf{H}_a \mathbf{K}_y \mathbf{H}_{ps} \mathbf{C}_{s_u} \mathbf{s}, \\ [\mathbf{C}_{s_u \mathbf{s}}]_{ij} &= \begin{cases} \sigma_s^2 & \text{if } i = (j-1)\ell_u + 1 \\ 0 & \text{else.} \end{cases} \end{aligned}$$

where \mathbf{H}_a , \mathbf{H}_{ps} and $\mathbf{\Gamma}$ represent the convolution matrices of the analog filters, the PS and the LPF at the receiver. Note that the diagonal elements of \mathbf{C}_y are not equal for $\rho \neq 0$ because of the non-stationarity of the process.

IV. RESULTS

After providing the expressions of the PS filter and the Eq optimized with respect to the MMSE criterion, we aim now at evaluating the performance of the designed 1-bit transceiver system in terms of the uncoded BER and bandwidth occupation. For the simulation, we assume for simplicity an AWGN channel, even though a general channel impulse response could be also handled by adapting the Eq design. On the other hand, the LPFs at the transmitter and receiver are implemented as Butterworth filter of fourth order with 3-dB bandwidth corresponding to the data-symbol rate. The length of the PS and of the Eq is $L_{ps} = 128$ and $L_{eq} = 64$ respectively and the roll-off factor is taken from the interval $(0, 1]$. In addition, we select the oversampling factors at both sides ℓ_u and ℓ_d from the set $\{2, 4, 8\}$. The performance measures in this work are

- the required SNR at uncoded BER of 10^{-3}
- and the bandwidth $B_{0.9375}$. The choice of this bandwidth is justified as follows. We consider the signal-to-interference-noise ratio (SINR), which is defined as $\text{SINR} = \alpha \frac{P_r}{\sigma_s^2 + \sigma_i^2}$, where σ_i^2 denotes the interference power of both adjacent channels spaced by $B_{0.9375}$ with the assumption that $\sigma_i^2 = 2\sigma_n^2$. For an SINR value of 10dB we get the 93,75% bandwidth $B_{0.9375}$:

$$\frac{\int_{f_c - B_{PA}/2}^{f_c + B_{PA}/2} S(f) df}{\int_{-\infty}^{+\infty} S(f) df} = 93.75\%, \quad (3)$$

where $S(f)$ is the power spectral density of the transmitter output signal $y_t(t)$. This bandwidth definition means that 93,75% of the signal power lies inside. The remaining 6.25% lying outside the defined bandwidth $B_{0.9375}$ is then considered as σ_i^2 .

A. Optimal fractional delay improves the performance

Fig. 3 shows the performance of the 1-bit system in terms of the required SNR at an uncoded BER of 10^{-3} and 93.75%-Bandwidth as function of the fractional delay Δn for $\ell_u = \ell_d = 2$ and for different roll-off factors ρ . One can observe that significant performance improvements are possible by tuning the fractional delay Δn . For small roll-off values adjusting Δn results in a compromise between the required SNR and the bandwidth while for higher roll-off values choosing Δn appropriately leads to the best performance for both criteria simultaneously. The minimal required SNR is achieved by the RRC filter with $\rho = 1$ and a fractional delay Δn between 0.2 and 0.6. We are 2.5dB far from the ideal unquantized case. If we look closer at

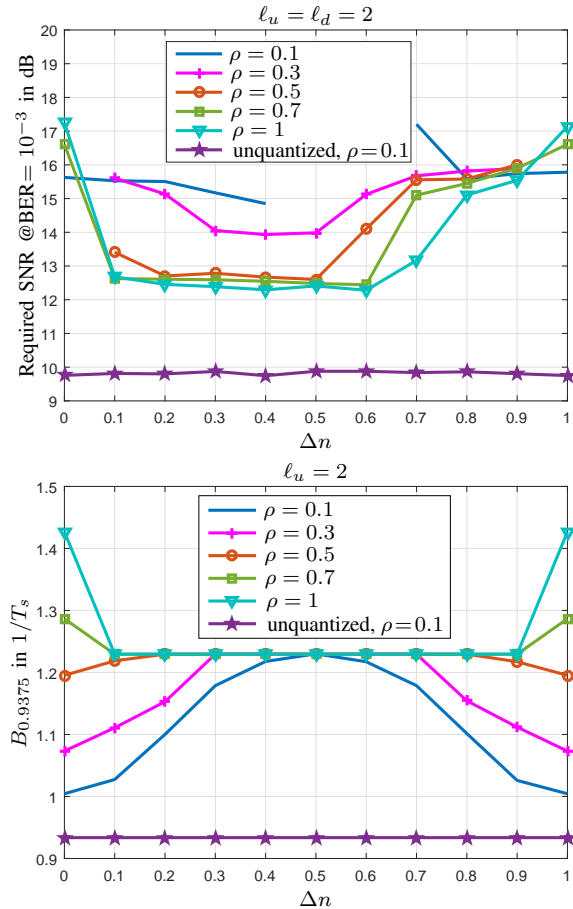


Fig. 3

REQUIRED SNR @ BER OF 10^{-3} AND 93,75% BANDWIDTH AS FUNCTION OF THE FRACTIONAL DELAY Δn FOR DIFFERENT ROLL-OFF FACTORS ρ AND FOR $\ell_u = \ell_d = 2$.

the discrete-time impulse response of the RRC filter with roll-off factor $\rho = 1$, $\Delta n = 0.5$ and with oversampling factor $\ell_u = 2$, depicted in Fig. 4, we observe a two-taps impulse response with unit weighting factors. At the output

of this special PS, we get each input symbol, which is a QPSK symbol, repeated twice. This implies that the input of the 1-bit DAC is a sequence of QPSK symbols which makes the non-linearity of the 1-bit DAC ineffective. Thus, we end up with a linear transmitter. We can get rid of the upsampling operation l_u and the PS in this special case, since their function is in any case realized by the sample and hold function of the DAC. Thus, the removal of the upsampling operation and the PS leads to a reduced system complexity without losing in the performance.

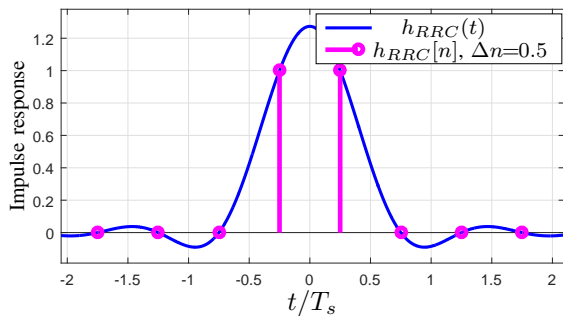


Fig. 4

DISCRETE-TIME RRC IMPULSE RESPONSE FOR $\Delta n = 0.5$; $\rho = 1$.

B. Oversampling improves the performance

In Fig. 5, we increase the oversampling factors to $l_u = l_d = 4$. In this case, the performance becomes less sensitive to the choice of Δn . The improvements in terms of bandwidth as well as required SNR are more obvious for small roll-off values. Similar conclusions can be drawn in Fig. 6 when increasing the oversampling factors to $l_u = l_d = 8$, where the performance gets very close to the ideal case. For better understanding of the influence of higher oversampling, we consider in Fig. 7 the case of $\rho = 0.1$ while increasing $l_d \in \{4, 8\}$ at receiver and keeping the transmit oversampling factor $l_u = 2$ on the one hand, and on the other hand we increase both oversampling factors simultaneously $l_u = l_d \in \{2, 4, 8\}$ at both ends of the communication link. It can be seen that the best SNR performance can be achieved with simultaneous oversampling $l_u = l_d = 8$ regardless of the fractional delay Δn . This result suggests that oversampling at both sides of the communication link is beneficial in terms of SNR performance for the 1-bit system, which can be explained by the fact that the quantization error is spread over higher bandwidth reducing the total noise power in the desired band.

C. Spectral shape

For illustration, Fig. 9 shows the power spectral density (PSD) of the 1-bit quantized signal after the LPF for different roll-off factors, while Fig. 8 depicts the corresponding PSD without quantization. Contrarily to the unquantized case, where oversampling can help relaxing the demands on the LPF, the spectral shape of the 1-bit system does not benefit from the oversampling. In fact, the spectral shape at the pass band region is mainly formed by the digital RRC filter, while the stop band is mainly influenced by the LPF. Thus it does not improve with higher oversampling factors.

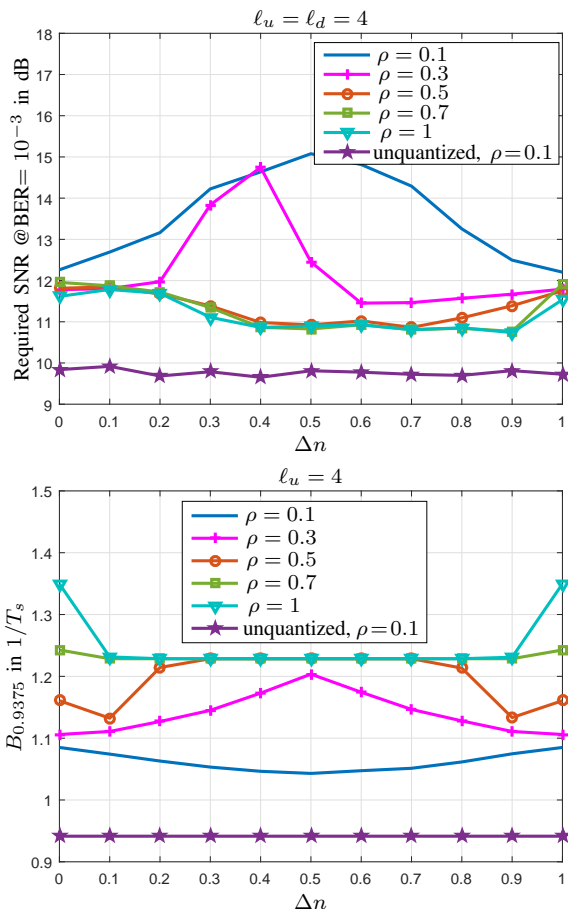


Fig. 5

REQUIRED SNR @ BER OF 10^{-3} AND 93.75% BANDWIDTH AS FUNCTION OF THE FRACTIONAL DELAY Δn FOR DIFFERENT ROLL-OFF FACTORS ρ AND FOR $l_u = l_d = 4$.

V. CONCLUSION

Low resolution ADCs and DACs are very advantageous in terms of the system complexity especially in the context of massive MIMO. Here, we considered a low cost single carrier communication system, where 1-bit DAC is applied to RRC spectrally shaped signals and 1-bit ADC is used at the receiver side. By tuning the fractional delay of the RRC impulse response and modifying the linear receiver to take into account the effects of coarse quantization, i.e. without any extra complexity, we have shown that the performance in terms of spectral efficiency and radiated power efficiency can be made quite close to the ideal system especially for moderate roll-off values. In addition, we have shown that oversampling beyond factor two is still beneficial especially for small roll-off values.

REFERENCES

- [1] Hien Quoc Ngo, E.G. Larsson, and T.L. Marzetta, "Energy and spectral efficiency of very large multiuser mimo systems," *Communications, IEEE Transactions on*, vol. 61, no. 4, pp. 1436–1449, April 2013.
- [2] S. Rangan, T.S. Rappaport, and E. Erkip, "Millimeter-wave cellular wireless networks: Potentials and challenges," *Proceedings of the IEEE*, vol. 102, no. 3, pp. 366–385, March 2014.

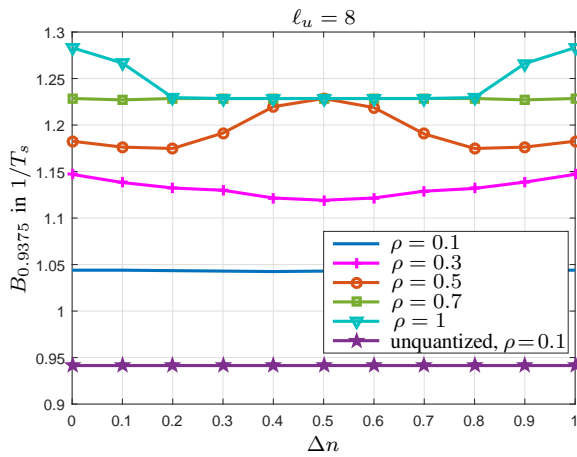
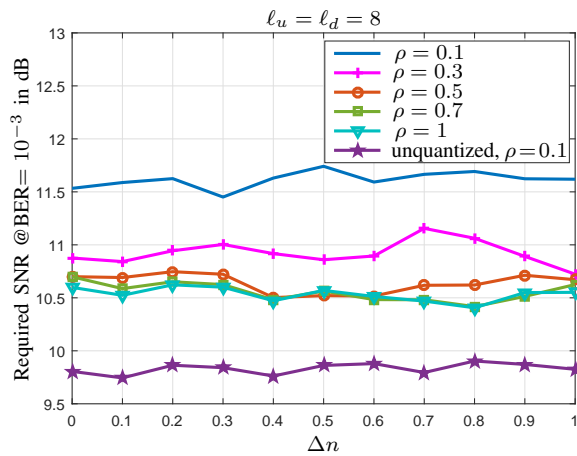


Fig. 6

REQUIRED SNR @BER OF 10^{-3} AND 93, 75% BANDWIDTH AS FUNCTION OF THE FRACTIONAL DELAY Δn FOR DIFFERENT ROLL-OFF FACTORS ρ AND FOR $l_u = l_d = 2$.

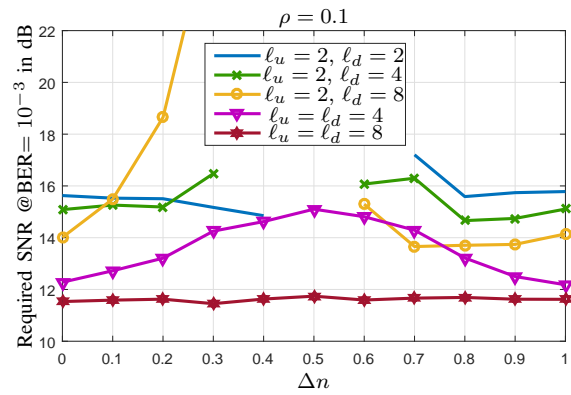


Fig. 7

REQUIRED SNR @BER OF 10^{-3} FOR $\rho = 0.1$ AND DIFFERENT OVERSAMPLING FACTORS AT THE TRANSMITTER AND THE RECEIVER.

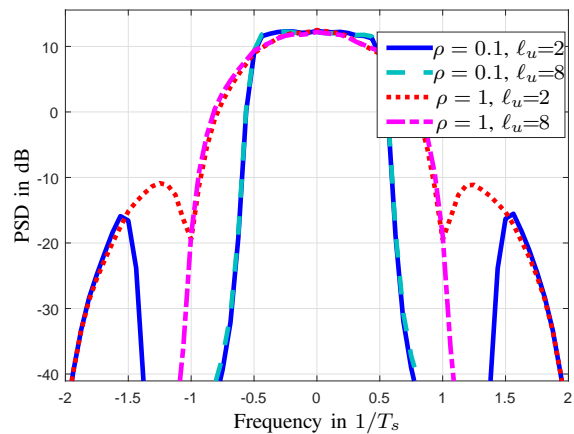


Fig. 8

PSD OF THE UNQUANTIZED SYSTEM

- [3] W. Roh, Ji-Yun Seol, JeongHo Park, Byunghwan Lee, Jaekon Lee, Yungsoo Kim, Jaewon Cho, Kyungwhoon Cheun, and F. Aryanfar, "Millimeter-wave beamforming as an enabling technology for 5g cellular communications: theoretical feasibility and prototype results," *Communications Magazine, IEEE*, vol. 52, no. 2, pp. 106–113, February 2014.
- [4] A.L. Swindlehurst, E. Ayanoglu, P. Heydari, and F. Capolino, "Millimeter-wave massive mimo: the next wireless revolution?," *Communications Magazine, IEEE*, vol. 52, no. 9, pp. 56–62, September 2014.
- [5] T.L. Marzetta, "Noncooperative cellular wireless with unlimited numbers of base station antennas," *Wireless Communications, IEEE Transactions on*, vol. 9, no. 11, pp. 3590–3600, November 2010.
- [6] E. Bjornson, L. Sanguinetti, J. Hoydis, and M. Debbah, "Optimal design of energy-efficient multi-user mimo systems: Is massive mimo the answer?," *Wireless Communications, IEEE Transactions on*, vol. 14, no. 6, pp. 3059–3075, June 2015.
- [7] E. Bjornson, J. Hoydis, M. Kountouris, and M. Debbah, "Massive mimo systems with non-ideal hardware: Energy efficiency, estimation, and capacity limits," *Information Theory, IEEE Transactions on*, vol. 60, no. 11, pp. 7112–7139, Nov 2014.
- [8] A. Mezghani and J.A. Nossek, "Belief propagation based mimo detection operating on quantized channel output," in *Information Theory Proceedings (ISIT), 2010 IEEE International Symposium on*, June 2010, pp. 2113–2117.
- [9] Jianhua Mo and R.W. Heath, "Capacity analysis of one-bit quantized mimo systems with transmitter channel state information," *Signal Processing, IEEE Transactions on*, vol. 63, no. 20, pp. 5498–5512, Oct 2015.
- [10] Jianhua Mo and R.W. Heath, "High snr capacity of millimeter wave mimo systems with one-bit quantization," in *Information Theory and Applications Workshop (ITA), 2014*, Feb 2014, pp. 1–5.
- [11] Jianhua Mo, P. Schniter, N. Gonzalez Prelcic, and R.W. Heath, "Channel estimation in millimeter wave mimo systems with one-bit quantization," in *Signals, Systems and Computers, 2014 48th Asilomar Conference on*, Nov 2014, pp. 957–961.
- [12] J. Singh, S. Ponnuru, and U. Madhow, "Multi-gigabit communication: the adc bottleneck," in *Ultra-Wideband, 2009. ICUWB 2009. IEEE International Conference on*, Sept 2009, pp. 22–27.
- [13] Shengchu Wang, Yunzhou Li, and Jing Wang, "Multiuser detection for uplink large-scale mimo under one-bit quantization," in *Communications (ICC), 2014 IEEE International Conference on*, June 2014, pp. 4460–4465.
- [14] C. Desset and L. Van der Perre, "Validation of low-accuracy quantization in massive mimo and constellation evm analysis," in *Networks and Communications (EuCNC), 2015 European Conference on*, June 2015, pp. 21–25.

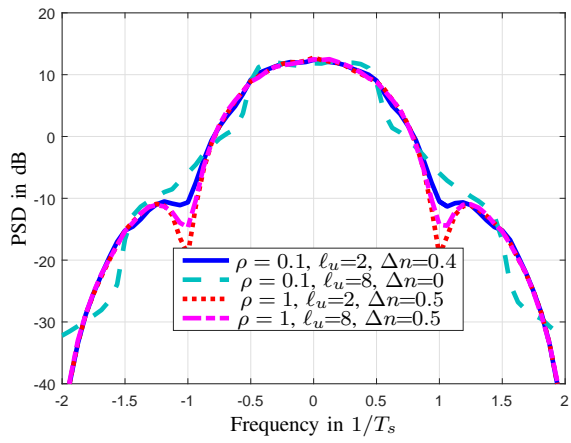


Fig. 9
PSD OF THE QUANTIZED SYSTEM